# Competition for space during bacterial colonization of a surface

# Competition for space during bacterial colonisation of a surface

Diarmuid P. Lloyd and Rosalind J. Allen
*SUPA, School of Physics and Astronomy, University of Edinburgh,*
*James Clerk Maxwell Building, Peter Guthrie Tait Road, EH9 3FD, Edinburgh, United Kingdom*

Competition for space is ubiquitous in the ecology of both micro-organisms and macro-organisms. We introduce a bacterial model system in which the factors influencing competition for space during colonisation of an initially empty habitat can be tracked directly. Using fluorescence microscopy, we follow the fate of individual *Escherichia coli* bacterial cell lineages as they undergo expansion competition (the race to be the first to colonise a previously empty territory), and as they later compete at boundaries between clonal territories. Our experiments are complimented by computer simulations of a lattice-based model. We find that both expansion competition, manifested as differences in individual cell lag times, and boundary competition, manifested as effects of neighbour cell geometry, can play a role in colonisation success, particularly when lineages expand exponentially. This work provides a baseline for investigating how ecological interactions affect colonisation of space by bacterial populations, and highlights the potential of bacterial model systems for the testing and development of ecological theory.

## Introduction

Spatial structure can have profound effects on the composition and dynamics of ecological communities. Ecological theory suggests that even in spatially uniform habitats, local neighbour interactions can lead to a variety of phenomena including competitor coexistence due to tradeoffs between life history strategies (e.g. between local competitive ability and dispersal)[1,2], community self-organisation[3], traveling waves of species dominance[4,5], and spatial variations in the prevalence of parasites or other traits[6,7]. Spatial variations in habitat type can produce even more varied ecological outcomes[8]. However, testing such predictions with well-controlled experiments on spatially-structured populations is often challenging (although not impossible[9]) for ecosystems consisting of macro-organisms, i.e. animals or plants.

Laboratory studies with microorganisms provide a way to test ecological theory that can overcome many of the practical issues associated with working with macro-organisms. While a large body of work exists for protist ecosystems[10,11], the potential of bacterial populations for testing ecological and evolutionary theory has only recently become widely recognised[12], as has the importance of using such theory to understand bacterial communities in the natural environment[13]. For bacterial populations, key studies have demonstrated the importance of spatial structure in promoting competitive restraint[14], maintaining coexistence in systems with cyclic dominance[15], favouring the evolution of toxins[16] and speeding up the evolution of antibiotic resistance[17–19]. Of particular interest are recent studies of range expansion, in which patterns of clonal dominance are visualised using fluorescently labelled strains of bacteria or yeast, as a population expands across the empty surface of an agar plate[20–22]. This work has shown that neutral fluctuations at the tips of expanding populations can have strong effects on genetic diversity[23,24]. These experiments provide a powerful tool for the testing and development of theory because fitness differences between strains can be measured with high accuracy, the spatial fates of different lineages can be tracked in detail, and the physical and ecological interactions between individual organisms are relatively simple[25–31]. The spatial patterns formed by expanding and competing bacterial lineages are also of interest in a synthetic biology context, where the aim is to produce controlled local patterns of differential gene expression[32].

In this paper, we use an experimental bacterial model system, combined with computer simulations, to address a different ecological scenario: the colonisation of an empty terrain by initially scattered individuals which proliferate to occupy contiguous patches, competing for space at the patch boundaries. This scenario is common in ecology; examples are to be found among lichens[33], algae[34], liverworts[35], vascular plants[9] and territorial animals[36]. In such a situation, where organisms compete locally for space (or, more generally, for resources), ecological theory points to several different processes that are at play[2,36,37]: expansion competition, in which a species captures space not already occupied by another, lottery competition, in which individuals compete to occupy space released when another dies, and overgrowth, or the capturing of space by direct competition at boundaries between species. For a particular ecosystem, a key task is to determine which of these mechanisms plays the major role. More generally, one would like to predict how the various mechanisms involved influence the spatial patterns of genetic mixing which emerge.

In our experiments, two fluorescently labelled strains of *Escherichia coli* bacteria compete locally for space, starting from an initially scattered configuration on an agarose surface. We track under the microscope the fates of hundreds of individual lineages, starting from individual "founder cells". In our system, cells do not die and are not motile, so that the key processes are expansion competition and direct competition at patch boundaries. By defining a measure of competitive success based on the final area occupied by a lineage, we can identify those lin-

eages that are "winners" and "losers", and determine the factors leading to their competitive success (or failure). We find that both expansion competition and boundary competition can play a role in colonisation success, with their relative importance being dependent on the founder cell density. More specifically, a picture emerges from our experiments, supported by our simulations, in which the competitive outcome is controlled by both founder cell lag time and "squeezing" between growing microcolonies at their boundaries. We also find that the emergent spatial patterns are density-dependent, with high initial cell densities typically leading to less uniformly shaped final patches. This study provides a baseline understanding of the factors that are at play when bacterial populations colonize soft surfaces, and a baseline methodology for investigating competition for space in microbial communities more generally.

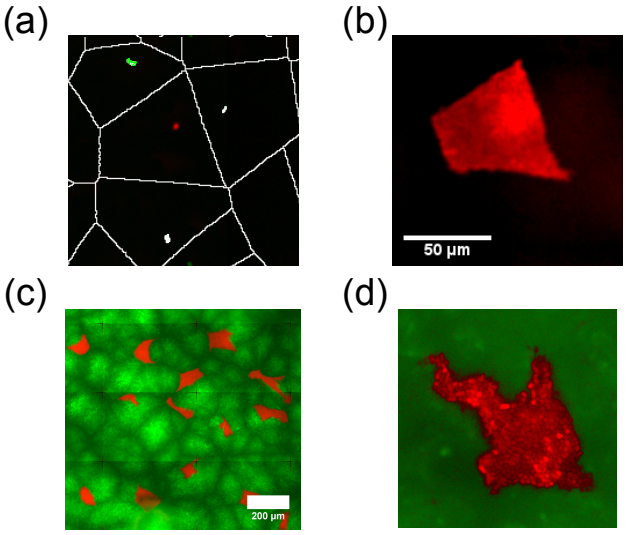


Figure 1: In our experiments, *E. coli* cells expressing two different fluorescent labels proliferate and compete for space. Cells expressing either cyan or yellow fluorescent protein are shown here as red and green respectively. (a) An initial configuration of progenitor cells on the surface; Voronoi polygons (white lines) are generated based on the positions of the progenitor cells. (b) A patch that results from the proliferation of one of the individual cells shown in (a); the surrounding patches are green (YFP rather than CFP) so do not appear on this image. (c) A montage of several microscope fields of view, showing how a complete picture of the colonised surface can be built. The red patches in these types of image are analysed to produce the results presented in this paper. (d) A detail of a patch arising in an experiment with an initially higher cell density, which shows a less uniform patch shape. In all images, the brightness levels have been adjusted in ImageJ for clarity.

## Results

### Visualising the fate of individual cell lineages

To track the fate of individual cell lineages during surface colonisation, we mixed two differently coloured fluorescently labelled strains of *E. coli* MG1655 (initially growing exponentially in liquid culture, see Methods) in a 1:19 ratio. A small volume of the mixed culture was spread evenly on the surface of a flat agarose pad containing nutrients and the sample was sealed with a glass coverslip. We used fluorescence microscopy to record the positions of over 1900 of these "founder cells" (Fig. 1a) across spatial regions up to $\approx 2 \times 10^5\,\mu\text{m}^2$. We then allowed the cells to proliferate during overnight incubation, so that the entire spatial domain became covered, before re-imaging (Fig. 1b-d). Fig. 1 shows typical results, with the minority and majority strains shown in red and green respectively. After the surface is colonised, distinct patches of red cells can be seen, each of which is surrounded by a "lawn" of green cells. Each red patch corresponds to space that has been occupied by the progeny of an individual red founder cell, in competition with the surrounding green cells. By analysing the sizes and shapes of the red patches, we can investigate the outcome of competition for space among the founder cells.

Fig. 1(b) and (d) show examples of individual red patches, in experiments with low (Fig. 1(b), $\rho_{\text{low}} = 1.5 \times 10^{-4}\,\text{cell}/\mu\text{m}^2$) and high (Fig. 1(c), $\rho_{\text{high}} = 7.2 \times 10^{-3}\,\text{cell}/\mu\text{m}^2$) densities of founder cells. For low founder cell density, we typically obtain patches with straight edges and clearly-defined corners. For high founder cell density, patch shapes tend to be more ragged.

### Quantifying winners and losers

To quantify the outcome of competition for space, we need to measure the extent to which a given cell lineage succeeds in outcompeting its neighbours. Starting from the initial configuration of founder cells, we assign a spatial "zone" to each founder cell by performing a Voronoi tessellation based on the founder cell positions (see Methods). Each cell's zone consists of the region of space that is closer to it than to any other founder cell[38]. This partitioning is illustrated in Fig. 1(a). As a null hypothesis, we suppose that, once the surface is colonised, the progeny of each founder cell will occupy the space defined by its zone. Comparing the shapes of the colonised patches which we observe in our experiments, we see that for low founder cell densities, there is indeed often a close correspondence between patch shape and the zones defined by the Voronoi tessellation (compare for example Fig. 1(a) and (b) which show the same region of space before and after colonisation). For high founder cell density, colonised patch shapes tend to deviate more from the shapes of the Voronoi zones (eg. Fig. 1(d)). A more detailed, quantitative analysis confirms that shapes of

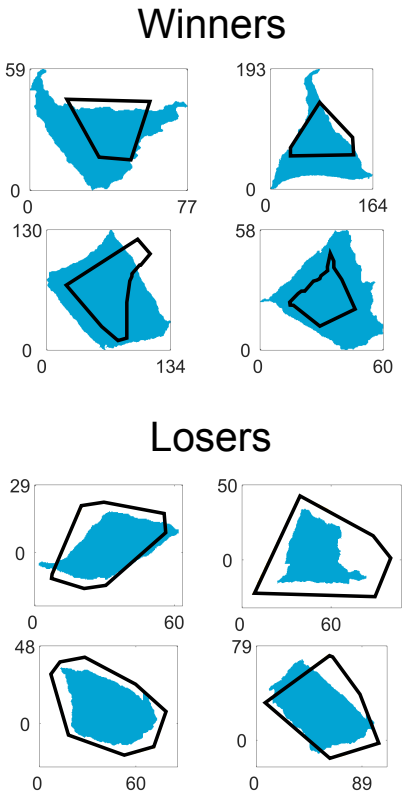


Figure 2: Shapes of selected patches resulting from "winner" and "loser" cells CAN WE WRITE WI VALUES ON THESE IMAGES? (blue), together with the shapes of their Voronoi zones (black lines). The blue shapes are obtained by thresholding the fluorescent images obtained after colonisation. These results are taken from the low cell density experiment ($\rho_{\text{low}}$ =1.5 × $10^{-4}$ cell/µm$^2$). Axes labels are microns.

the colonized patches and of the corresponding Voronoi zones correlate more strongly at low founder cell density than at high founder cell density (Fig. S7).

To identify those cells which are "winners" and "losers" in the competition for space, we define a quantity which we call the "winner index" W.I.. This is the ratio between the colony patch area which arises from a given founder cell, and the area of its initial Voronoi zone:

$$\text{W.I.} = \frac{A_{\text{P}}}{A_{\text{V}}}, \tag{1}$$

where $A_{\text{P}}$ is the final patch area arising from a given founder cell, and $A_{\text{V}}$ is the area of its Voronoi zone. A value W.I. = 1 corresponds to a cell whose lineage has colonized only the space closest to it. "Winners", or cells which colonize more space than that closest to them, will have W.I. > 1, while "losers", which colonise less space that that closest to them, will have W.I. < 1. Eq. 1 does not, of course, provide the only possible definition of competitive success; however, we find that our qualitative conclusions are not sensitive to the precise definition of the winner index (see Supplementary Information).

Figure 2 illustrates the shapes of the colonisation patches (blue) of several "winner" and "loser" cells, together with the shapes of their Voronoi zones (black lines), in an experiment with an initially low cell density ($\rho_{\text{low}}$ =1.5 × $10^{-4}$ cell/µm$^2$). These images do not reveal any obvious "winning or losing strategy"; for example while some winners seem to have gained territory by pushing out from their corners (upper 2 winners in Fig. 2), others seem to have expanded more uniformly beyond their Voronoi zones (lower 2 winners in Fig. 2).

Fig. 3(a) and (b) show the distribution of W.I. values obtained in our experiments, for founder cells at high and low initial cell densities respectively. In both cases, the distribution of W.I. values is peaked around W.I. = 1, but we also observe significant numbers of winners and losers. Comparing the results for low and high founder cell densities (Fig. 3(a) and (b)) we see that the distribution is broader at high founder cell density. For high founder cell density ($\rho_{\text{high}}$ =7.2 × $10^{-3}$ cell/µm$^2$), the log normal coefficient of variation ($c_{\text{v}}$, ) was $c_{\text{v}}$ = 0.54; in contrast, for the low founder cell density experiment, $c_{\text{v}}$ = 0.27. Thus, when the founder cell density is high, such that expanding lineages collide earlier, we obtain more deviation from the Voronoi patch shape (Fig. S7 and also Fig. 1 b and d), and also observe more extreme effects of competition for space (i.e. more winners and correspondingly more losers).

### Expansion competition can play a significant role

Ecological theory suggests that two competitive processes are likely to be important in determining the outcome of our experiments: expansion competition, in which clonal lineages "race" to occupy empty space, and direct competition at the boundaries between neighbouring patches[2,36,37].

#### *Tracking the early stages of surface colonization*

To determine the role of expansion competition in our experiments, we measured the growth behaviour of individual cell lineages (microcolonies) in the early stages of growth, i.e. prior to collision with their neighbours, using time-lapse microscopy. We measured the lag time, or waiting time before a founder cell starts to divide[39], and also tracked the rate of microcolony expansion, once a founder cell had started to proliferate. In agreement with others' observations[40–42], we observed significant variability in lag times among founder cells (Fig 4(a), mean $t_{\text{lag}}$ =53 min, with a standard deviation of 16 min). The expansion rates of growing microcolonies show much less variability: tracking the microcolony expansion rate as a function of microcolony size, we find that this varies

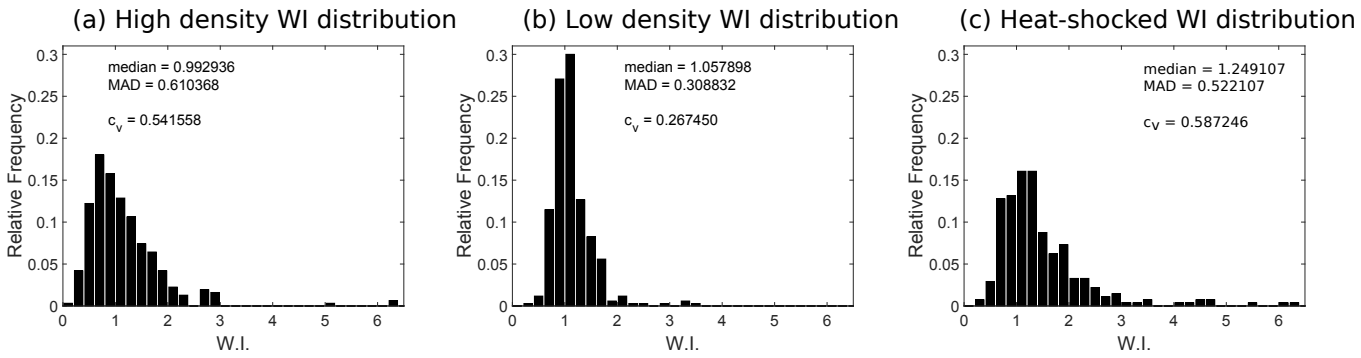


Figure 3: The distribution of winner index values across cells in the population is affected by our experimental conditions. Winner index distributions are shown for the following experiments: (a) High initial cell density ($\rho_{\rm high}$ =$7.2 \times 10^{-3}$ cell/µm$^2$), exponential growth, $N = 274$. (b) Low initial cell density ($\rho_{\rm low}$ =$1.5 \times 10^{-4}$ cell/µm$^2$), exponential growth, $N = 340$. (c) Heat-shocked cells, low initial cell density ($\rho_{\rm low}$ =$1.5 \times 10^{-4}$ cell/µm$^2$), $N = 313$. Two measures of distribution width are quoted in the panels: the median absolute deviation (MAD) and log-normal coefficient of variation ($c_{\rm v}$).

somewhat during the first few divisions, but thereafter the microcolonies expand exponentially with a mean area doubling time of 20.0 min and standard deviation of 2 min. In agreement with others[31], we also observe a transition between two growth regimes, each with a different expansion rate, at a microcolony size of about $5.3(8) \times 10^3$ µm$^2$; this has been shown to correspond to cells beginning to penetrate the agarose forming a second vertical layer (see Supplementary Information). For simplicity, our definition of winner index does not take this vertical stacking into account; although it would be interesting to include it in future work.

*Manipulating lag times allows us to probe the effects of expansion competition*

Since founder cell lag times are more variable than micro-colony expansion rates in our experiments, we expect differences in the lag times of individual founder cells to be the dominant factor controlling expansion competition. To test the effect of lag-time variability, we manipulated the lag-time probability distribution. This can be achieved by using founder cells taken from the stationary phase of growth in liquid culture, which have been exposed to a sub-lethal heat shock (for 15 min), prior to deposition on the agarose surface (see Methods). This treatment has been shown in previous work to increase both the mean and variance of bacterial lag times[43–45], and this was indeed the case in our experiments (Fig. 3(a), compare to Fig. 3(b)).

*Broader lag-time distribution produces more winners and losers*

If expansion competition is a significant factor in our experiments, we would expect that the broader lag-time distribution for heat-shocked founder cells should result in a broader distribution of W.I. values, with a higher proportion of lineages that either out-compete their neighbours (due to relatively short lag times) or are out-competed by their neighbours (due to relatively long lag times). Thus, we expect our measure of W.I. distribution dispersion, $c_{\rm v}$, to be larger for the heat-shocked cells than for those deposited on the surface in the exponential phase of growth. This was indeed the case, as shown in Fig 3: for heat-shocked founder cells we observed that, for a founder cell density of $1.5 \times 10^{-4}$ cell/µm$^2$, $c_{\rm v} = 0.59$, compared to $c_{\rm v} = 0.27$ for the exponentially-growing founder cells at the same cell density (compare the W.I. distributions in Fig 3, panels b and c).

**Boundary competition is significant at high cell densities**

Direct competition at the boundaries between colliding microcolonies may also be an important factor in our experiments. At these collision boundaries, local competitive interactions could, in principle, involve secretion of toxins or bacteriophage, extracellular polymeric substances or antibiotics[46]. For *E. coli* MG1655, however, cell-cell interactions within growing microcolonies on agarose surfaces are believed to be mainly mechanical – *i.e.* generated by physical pushing of the cells against each other, and by physical interactions between the cells and the agarose surface (as well as the glass cover slip)[25–31]. These mechanical interactions are expected to generate pushing forces between neighbouring patches as they collide, influencing the final colony shape.

*Correlating winner index with local neighbour geometry provides a probe of boundary competition effects*

If boundary competition is a significant factor in our experiments, then we would expect the local geometry of

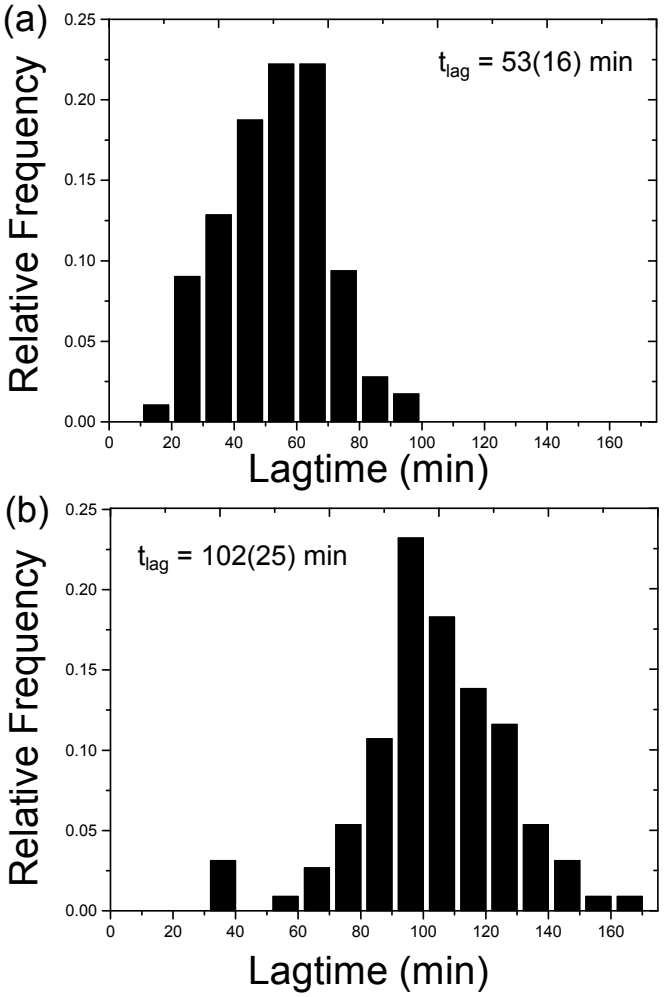


Figure 4: Founder cell lag times are broadly distributed and the width of the distribution can be manipulated by pre-treating the cells. Lag-time distributions are shown for (a) initially exponentially growing cells and (b) stationary-phase cells exposed to 50 °C 15 min heat-shock prior to deposition on the surface. Mean lag-times and their standard deviations are given in each panel. The heat-shocked cells show a longer average lag time and a broader distribution of lag times. THE INSERT IS GOOD BUT ITS A BIT AMBIGUOUS: COULD WE WRITE IN THE PANEL MEAN = SD = ? ALSO COULD WE PUT A HEADING ON THE GRAPHS LIKE IN FIG 3?

the neighbours of a given founder cell to affect its eventual success. This local neighbour geometry is captured in the geometry of a founder cell's Voronoi patch - thus, by looking for correlations between Voronoi patch geometry and winner index, we can investigate the influence of boundary competition in our experiments.

As a basic hypothesis, one might expect the *area* of the Voronoi patch to play an important role. On the one hand, cells with small patches need to gain less absolute area to achieve a large winner index (since W.I. depends on the relative area). On the other hand, however, founder cells with large patches can produce large microcolonies, which might exert a greater pushing force upon collision. One might also expect the *shape* of a cell's Voronoi patch to be significant, since this reflects the number and geometrical arrangement of neighbouring founder cells, which should affect the force balance at the boundary between colliding microcolonies. We therefore looked for correlation between the eventual success of a given founder cell (as measured by its W.I. value) and both the size and shape of its Voronoi patch.

*Founder cells with small Voronoi patches tend to be winners*

Our analysis showed that cells with smaller patches tended to have a higher average winner index (Fig 5). This was true for both the initial cell densities tested (in both cases for exponentially-growing founder cells), although for the higher density ($\rho_{\mathrm{high}} = 7.2 \times 10^{-3}\,\mathrm{cell}/\mu\mathrm{m}^2$, Fig. 5(a)), the trend was clearer. As discussed above, cells with smaller patches may tend to be winners simply because W.I. is a relative measure, so that cells with smaller patches need to gain less absolute area to be declared "winners". HAVE WE TESTED OTHER MEASURES IN THE SI? IF SO COULD COMMENT ON THAT HERE. However, a correlation between patch size and winner index may also reflect the typical shapes of microcolonies when they collide. Since early-stage microcolonies are typically more anisotropic than late-stage microcolonies (see supplementary material), lineages with small Voronoi patches are likely to be more anisotropic when they collide with their neighbours. This might prove advantageous in "squeezing between the gaps" between colliding neighbouring microcolonies. Interestingly, we did not observe any advantage for founder cells with large Voronoi patches, even though these might be expected to generate a greater pushing force upon collision. We speculate that this is because larger microcolonies tend to have already "buckled" into the vertical direction when they collide. In this case, newborn cells can be accommodated in layers, reducing the horizontal outward pressure within the microcolony[31].

*Voronoi patch shape differs between winners and losers*

To explore the effects of Voronoi patch shape, we also characterized the shapes of individual patches, by computing their Fourier descriptor spectra[47]. The Fourier descriptor spectrum of a given shape is a list of numbers (Fourier descriptor magnitudes) which describe the amplitudes of different Fourier modes associated with the perimeter of the shape (for details see Methods). The Fourier descriptor spectrum of an object depends only on its geometrical shape (it is independent of scaling, translation or rotation[47]). Thus, we can describe the shapes of the Voronoi patches corresponding to individual founder cells by their Fourier descriptor spectra. Im-

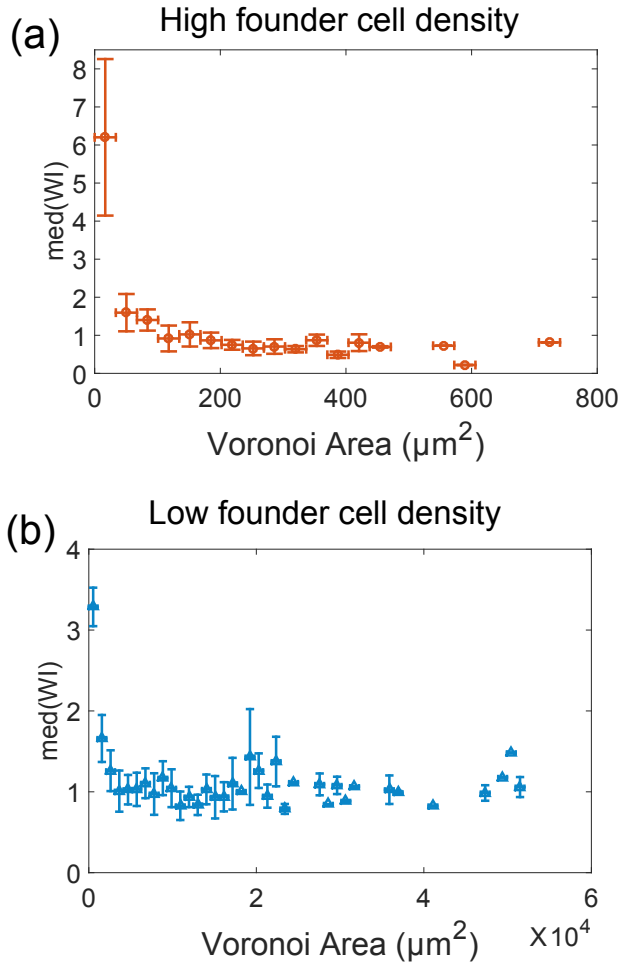


Figure 5: Cells with smaller initial patches are more likely to be winners. Median WI values are shown as a function of Voronoi patch size for (a) an experiment at high founder cell density ($\rho_{\text{high}}$ =7.2 × 10$^{-3}$ cell/μm$^2$), and (b) an experiment at low founder cell density ($\rho_{\text{low}}$ =1.5 × 10$^{-4}$ cell/μm$^2$). In both cases, founder cells were taken from exponential culture.

portantly, this allows us to conveniently quantify the *difference* in shape between two Voronoi patches, by computing the Euclidean distance between their Fourier descriptor spectra (see Methods). We used this method to test for differences in the geometrical characteristics of winning versus losing Voronoi patches. Fig. 6 shows our results, in the form of multi-dimensional scaling (MDS) plots for the high and low founder cell density experiments (Fig. 6a and b respectively). An MDS plot projects the multidimensional matrix of shape differences between all pairs of patches onto two dimensions. In these plots, each point represents a founder cell Voronoi polygon and the distance between two points represents, as closely as possible, the dissimilarity between their shapes (as measured by the Euclidean distance between their Fourier descriptor spectra). Thus, founder cell points that are shown close together are similar in their Voronoi patch shapes while those that are far apart are different in their Voronoi patch shapes. In these plots, we have separated winners and losers by colour; the red points represent founder cells that eventually become "losers" - i.e. those whose eventual W.I. is in the lowest 10% of the population, and the blue points represent founder cells that go on to become "winners" - i.e. those whose eventual W.I. is in the highest 10% of the population. Clustering among either red or blue points in the plot would indicate a "typical" Voronoi patch shape for either losers or winners.

Fig. 6 shows that we do indeed observe clustering between Voronoi patch shapes for eventual winners and losers (distinct red and blue clusters of points), for both the high and low founder cell density experiments (Fig. 6a and b respectively), although the clustering is more marked in the high density case. The statistical significance of this apparent clustering can be measured using multivariate ANOVA[48] (PERMANOVA; see Methods); this showed a significant distinction between the winner and loser points for both the high density experiment (p=0.001) and the low density experiment (p=0.008). This supports our hypothesis that there are indeed geometrical features of the neighbour configuration that predispose founder cells towards success or failure in the competition for space, irrespective of patch size, even though these features are not immediately apparent on visual inspection of winner and loser Voronoi patches (see, e.g. Fig. 2).

### Simulations reproduce our experimental results

Our experimental results suggest that the eventual success of a given cell lineage in out-competing its neighbours depends on both the lag time before the founder cell begins to divide, and on the size and shape of the founder cell's Voronoi patch, defined by its neighbours. To verify this picture, and to further investigate the interplay between these two factors, we performed computer simulations of a simple model.

In our simulations, the spatial habitat is represented by a 2-dimensional square lattice of 500×500 sites. We assume that each site can be occupied by a single bacterial cell. Upon reproduction, a cell retains its original site and also produces a progeny cell which occupies a previously empty site; thus each founder cell gives rise to a microcolony which expands in space. The simulation algorithm is described in detail in Methods. Briefly, at the start of the simulation, randomly chosen sites are populated by founder cells. Each founder cell begin to reproduce after a waiting time which is chosen from one of our experimental lag time distributions (Fig. 4). The age at which a cell reproduces is chosen from a uniform distribution with range 18 min-22 min (based on experiments tracking the area growth of colonies on 3 %agarose at early times). Upon reproduction, the progeny cell is placed at random into any of the 8 sites surrounding its parent (i.e. the Moore neighbourhood), if empty. In most

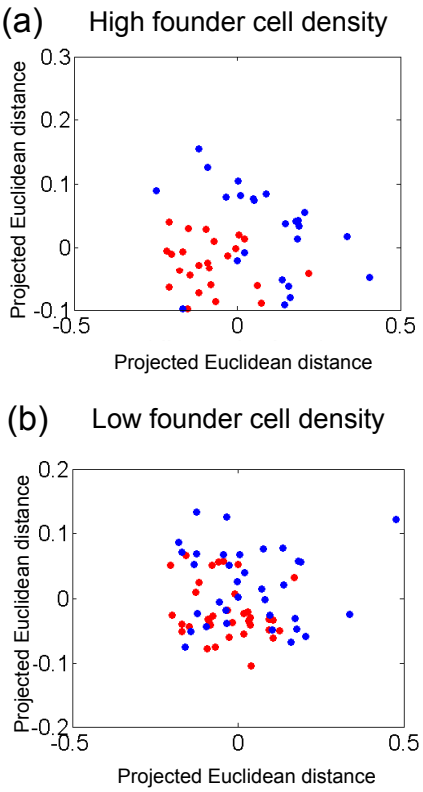


Figure 6: Founder cells that go on to be winners are statistically different in Voronoi patch shape from those that go on to become losers. Multidimensional scaling plots provide 2d projections of the matrix of differences in Fourier descriptor spectra among individual Voronoi patches. Red points represent cells that go on to be losers (bottom 10 % of the W.I. distribution), and blue points those that go on to become winners (top 10 % of the W.I. distribution). Distinct clusters of red and blue points indicate distinct typical Voronoi patch shapes for losers and winners. The statistical significance of this clustering was analysed by PERMANOVA (see Methods). (a) Results for high initial cell density, (clustering significance by PERMANOVA: $p = 0.001$). (b) Results for low initial cell density, (clustering significance by PERMANOVA :$p = 0.008$. I THINK THERE SHOULD BE STRESS VALUES ON THESE PLOTS, DO THESE COME OUT OF MATLAB? THEY MEASURE HOW GOOD THE 2D PROJECTION IS. ALSO FOR THE PERMANOVA IT WOULD BE GOOD TO REPORT THE NUMBER OF DATA POINTS

of our simulations, if none of these sites is empty, the progeny cell is instead placed on the perimeter of the microcolony. This mimics the fact that in our experiments, birth of new cells deep within the microcolony pushes existing cells outwards, expanding the microcolony area. If the microcolony becomes completely blocked by neighbouring cells, i.e. there are no empty lattice sites at its perimeter, its growth ceases. To mimic a scenario where cell growth could be inhibited deep within the colony (e.g. by nutrient limitation), we also carried out some simulations in which progeny cells could only be placed in sites surrounding the parent. We term these two scenarios "exponential area growth" and "perimeter growth", respectively.

Our simulations allow us to investigate systematically the role of expansion and boundary competition. By adjusting the lag time distribution, we can control the extent of expansion competition. By adjusting the founder cell density we can mimic our experiments at low and high density and control the extent of boundary competition. Finally, by switching between the "exponential" and "perimeter" growth regimes, we can vary the strength of "pushing" interactions between microcolonies once they have collided.

Because the microcolony area is observed to increase exponentially in our experiments FIGURE?, we begin with the exponential area growth regime, in which progeny cells are placed at colony boundaries if the Moore neighbourhood of their parent is full.

*Effects of expansion competition*

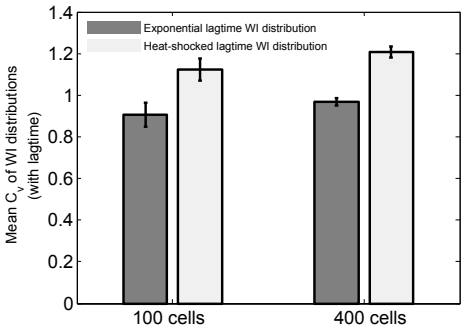


Figure 7: A broader lag-time distribution produces a broader winner index distribution, in our simulations as in our experiments. The log-normal coefficient of variation ($c_v$) of the WI histograms is shown for simulations using different lagtime distributions and initial seed cell densities. Using the heat-shocked lag-time distribution (taken from our experimental data, Fig. 4b) results in a wider WI distribution than using the exponential lag-time distribution (Fig. 4a). This result holds for two different founder cell densities, 100 initial cells (i.e. $4\times\ 10^{-4}$ cells per site) and 400 initial cells (i.e. $1.6\times\ 10^{-3}$ cells per site). In all cases, simulations are performed in the exponential area growth regime.

We first tested whether our simulations could reproduce our experimental observation that a broader lag time distribution led to a broader distribution of winner index values (Fig. 3). To this end, we performed simulations (in the exponential area growth regime) with lag times sampled from our two experimental distributions: the lag time distribution for exponential phase founder cells (Fig. 4a), and that for heat-shocked founder cells (Fig. 4b). As expected, we observed a wider distribution of W.I. values for the simulation with the broader (heat-shocked) lag time distribution (Fig. 7). In our simulations, we are also able to correlate the lag times of individual founder cells with their eventual fate (i.e.

their W.I. value)[49]. This analysis showed that indeed those cells with shorter lag times had, on average, higher values of the winner index (Fig. S7). DO WE ALSO REFER TO OTHER SI FIGS? THEY ALL SEEM TO BE FIG 7? NEED TO MAKE SURE ALL FIGURES IN THE SI GET REFERENCED SOMEWHERE IN MAIN TEXT

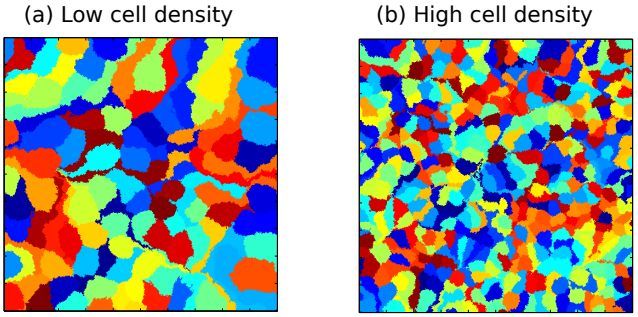


Figure 8: Snapshots of final simulation configurations, for simulations with no lag times, in the exponential area growth regime. In both panels, the lattice is 500x500 sites, with either (a) 100 seed cells or (b) 400 seed cells.

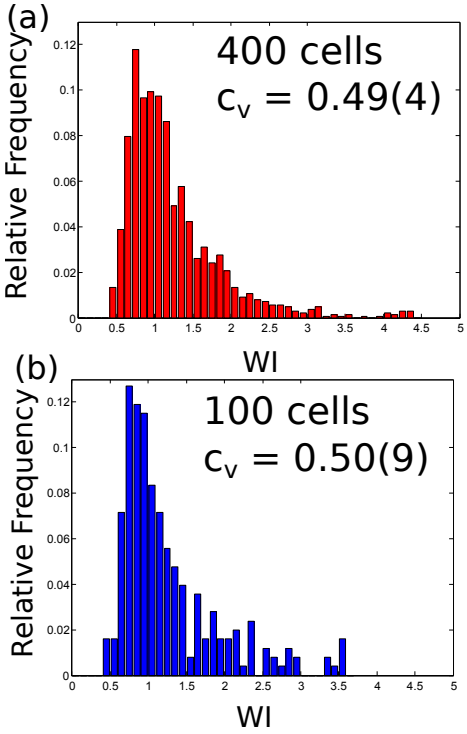


Figure 9: Simulations without lag times produce a spread of winners and losers, suggesting that boundary competition is important. W.I. distributions are shown for simulations in the exponential area growth regime, without lag times, for two founder cell densities: (a) N=400 seed cells, (b) N=100 seed cells.

*Effects of boundary competition*

In our simulations, we also eliminate the effects of expansion competition, by allowing all the founder cells to divide from the start of the simulation (i.e. removing the lag times, so that all colonies expand at equal exponential rates from the start). This allows us to investigate the effects of boundary competition in isolation. Fig. 8 shows typical snapshots of the final configuration from such simulations (with different microcolonies coloured differently). In these simulations, final colony shapes are typically irregular, suggesting that there is an effect of "pushing" at the boundaries between colliding colonies. This is also apparent in the winner index distributions for these simulations (Fig. 9), which are broad, showing that boundary competition has created significant numbers of winners and losers.

Repeating our analyses of Voronoi patch size and shape, we find that, as in our experiments (Fig. 5 and Fig. 6), in our simulations, founder cells with smaller Voronoi patches tended to be successful (Fig. 10), and there is clear clustering between the shapes of the Voronoi patches corresponding to "winning" and "losing" founder cells (Fig. 10, statistically significant clustering of winners and losers, p=0.001 for both low and high density simulations).

Interestingly, however, founder cell density seems to have a slightly different effect in our simulations compared to our experiments. In the experiments, the distribution of winner index values was broader for experiments at high founder cell density, compared to low founder cell density (Fig. 3a and b), and we also observed a more pronounced effect of Voronoi patch size and shape at high founder cell density, compared to low founder cell density (Fig. 5 and Fig. 6); although the effect of shape was statistically significant in both cases. In contrast, in the simulations, the distributions of W. I. values are similar in width for simulations at low and high founder cell density ($4 \times 10^{-4}$ cell/site and $1.6 \times 10^{-3}$ cell/site, or 100 and 400 initial seed cells respectively), and we observe similar effects of Voronoi patch size and shape for the two founder cell densities (Fig. 10, left and right panels). One possible explanation for this might be that in the experiments, colonies that collide when they are small (as in the case of high founder density) are still growing strictly as a single layer in the horizontal plane, whereas colonies that collide when they are larger (as in the case of low founder cell density) are already growing as multiple layers[31], so exert reduced pushing forces in the horizontal plane. This factor is not taken into account in the simulations, but could be tested in future work.

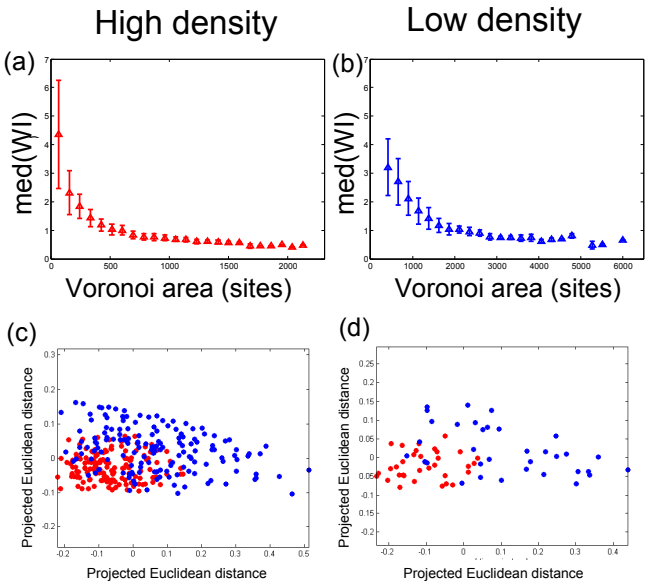


Figure 10: Simulations without lag times in the exponential area growth regime show similar effects of Voronoi polygon size and shape as in our experiments. (a,b) Median W.I. values are plotted as a function of binned Voronoi polygon area, for simulations with 400 (a) and 100 (b) founder cells. (c,d) MDS plots showing the similarity between Fourier spectra of Voronoi polygons in the top (blue,'winners') and bottom (red,'losers') 10 % of the relevant W.I. distributions, for simulations with 400 (c) and 100 (d) founder cells. In both cases, clustering among the red and blue points is statistically significant (PERMANOVA: $p = 0.001$ for both low and high founder cell densities. GIVE NUMBERS OF DATA POINTS TOO. AND STRESS VALUES?

### "Pushing" interactions between microcolonies play an important role in boundary competition

In our simulations, we can change the way that microcolonies interact at collision boundaries, by switching between the "exponential area growth" and "perimeter growth" regimes. In the former regime, microcolonies that collide will continue to grow exponentially, adjusting their shape to fit between the gaps until each microcolony is completely surrounded. In the latter regime, growth is locally inhibited at collision boundaries such that colliding microcolonies slow, and eventually stop, their growth. This regime might correspond to a case where nutrient penetration to the inner parts of the colony is a limiting factor[30], or might loosely mimic a case where colonies grow in several stacked layers[31].

Repeating our simulations in the perimeter growth regime (again in the absence of lag times), we obtain quite different results. Fig. 11 shows typical final snapshots from our simulations, for the same parameters as in Fig. 8, but in the perimeter growth rather than the exponential growth regime. Comparing Fig. 11 with Fig. 8, we see that in the perimeter growth regime, the final patch shapes are more regular, corresponding more

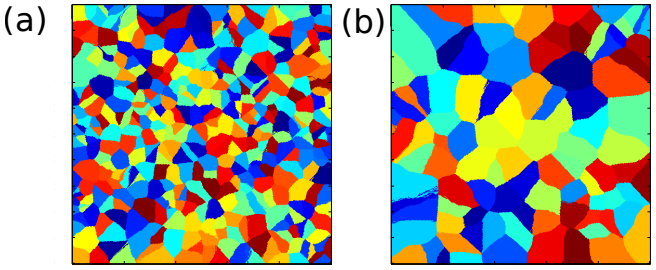


Figure 11: Snapshots of final simulation configurations, for simulations with no lag times, in the perimeter growth regime. In both panels, the lattice is 500x500 sites, with either (a) 100 seed cells or (b) 400 seed cells. THE RIGHT-LEFT ORDER IS SWAPPED WITH RESPECT TO FIG 8, CAN WE CHANGE IT ROUND?

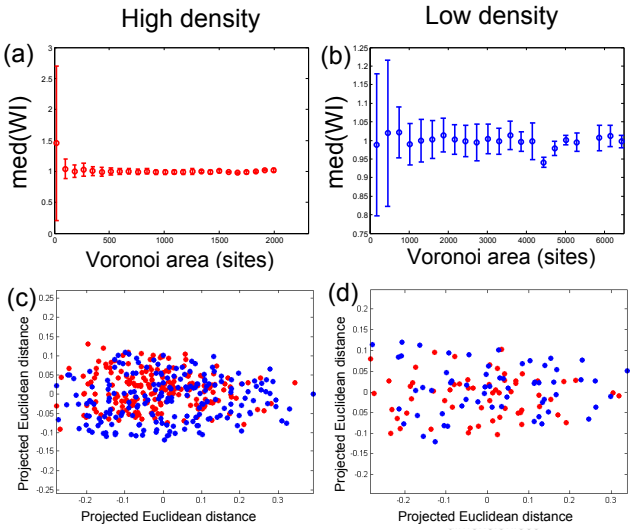


Figure 12: Simulations without lag times in the perimeter growth regime do not show significant effects of patch area or shape on winner index. (a,b) Median W.I. values are plotted as a function of binned Voronoi polygon area, for simulations with 400 (a) and 100 (b) founder cells. (c,d) MDS plots showing the similarity between Fourier spectra of Voronoi polygons in the top (blue,'winners') and bottom (red,'losers') 10 % of the relevant W.I. distributions, for simulations with 400 (c) and 100 (d) founder cells. In both cases, clustering among the red and blue points is not statistically significant (PERMANOVA: $p = 0.135$ for high founder cell density and $p = 0.202$ for low founder cell density). GIVE NUMBERS OF DATA POINTS TOO. AND STRESS VALUES?

closely to the Voronoi polygon areas associated with the founder cells. Analysing the effects of Voronoi patch size and shape on the final outcome of competition in this regime (Fig. 12), we also find that neither patch size nor shape are significant factors in distinguishing winners from losers (contrast Fig. 12 with Fig. 10). These results suggest that microcolony "squeezing" at the boundaries of colliding colonies may be responsible for the boundary competition effects (e.g. effects of Voronoi polygon size and shape) that we see in our experiments.

## Discussion

In this paper, we have used a bacterial model system to investigate the ecological factors influencing competition for space as an initially scattered population colonizes a spatial domain. Our study has focused on a "simplest possible" model system, in which the competing populations are identical (except for their fluorescent markers) and death, dispersal and complex ecological interactions are all absent. For this system, we can track the fates of individual founder cells as they proliferate, allowing us to define a simple measure of the outcome of competition, which we term the "winner index". Quantifying success in this way allows us to investigate in detail the factors that influence the outcome of competition for space, at the level of individual founder cells.

In our experimental system, competition for space involves expansion competition, manifested as differences in the founder cell lag times, and boundary competition, manifested as "pushing" interactions between growing microcolonies as they collide at their boundaries. The former is detectable in an effect of changing the lag time distribution (which we achieve by heat-shocking the founder cells, and the latter is detectable in the form of correlations between the founder cell's neighbour geometry and its eventual success. We find evidence for the importance of both these competitive mechanisms, but boundary competition shows more pronounced effects when the experiment is initiated with a high founder cell density, such that colonies collide when they are smaller. We speculate that this may be because small colonies are typically expanding asymmetrically and exponentially, in a single horizontal plane, whereas larger colonies are typically more symmetric in shape, may be nutrient-limited in their centres (although this is unlikely in our experiments) and are likely to consist of several layers of cells.

Importantly, we are able to reproduce the key features of our experiments using computer simulations of a simple model which includes only patch expansion (with a lag time) and exclusion between microcolonies at their boundaries. In our simulations, we can manipulate the growth rules to favour either expansion or boundary competition. Eliminating "squeezing" of microcolonies as they collide with their neighbours, by restricting cell proliferation to the perimeter of expanding microcolonies, drastically decreases the effects of boundary competition in our simulations.

Our study is intended as a starting point in investigating competition for space among expanding microbial populations, and as such, naturally involves technical aspects that warrant further discussion. Firstly, our definition of the winner index, as the area covered by a given cell lineage at the end of the experiment, relative to its Voronoi polygon, is somewhat arbitrary. One might prefer to measure the difference between the microcolony area and the Voronoi patch size, or normalise the success measure by average Voronoi patch size rather than individual Voronoi patch size. NEED SOME SENTENCE HERE ON THE EFFECTS OF THIS? IS THERE SOMETHING IN SI WE CAN REFER TO HERE? Secondly, here we chose to end our analysis soon after the whole surface was colonised (*i.e.* after ≈16 h); one might wonder whether our results might change over a longer timescale, as cells continue to interact at microcolony boundaries. This would certainly be interesting but from a practical point of view, very long timescale experiments are difficult due to the tendency of the agarose pad to dry out. Thirdly, it is important to note that for larger microcolonies, a second layer of cells forms prior to collision with the neighbours; i.e. growth is occurring to some extent in the vertical as well as horizontal direction[31]. This is not taken into account in our definition of the winner index. One could perhaps include it by measuring total fluorescence rather than patch area, or by performing confocal microscopy, but both involve their own technical challenges.

Despite these challenges, our results do provide a clear picture of the ecological factors influencing competition for space in this system. One of the interesting results that emerge from our study is that at low founder cell density, the patches colonized by individual lineages are in the main remarkably similar to the Voronoi patches corresponding to the founder cell neighbour configurations (Fig 1). This is by no means an obvious outcome, since growing *E. coli* microcolonies are essentially granular materials, with complex internal cell orientations[25–31], which should lead to complicated force balances upon collision with neighbouring microcolonies. Indeed, some other studies of similar systems have reported "fractal-like" patterns, in which colliding lineages form elongated, intertwined domains[21,32]. Although we do see greater deviation between final and Voronoi patch shapes at higher founder cell densities (Fig 1), we do not observe fractal-like patterns, even at very high founder cell densities. Although this requires further investigation in future work, our setup does differ from previous studies[21,32] in that the growing populations are confined by a glass cover slip which exerts a vertical pressure on them. If this does turn out to be important in determining the patterns formed, this would be an interesting manifestation of the importance of physical interactions (such as elasticity and friction) in determining the outcome of bacterial community organisation[30,31].

To what extent can the approach described here be used to understand spatial competition in more complex ecological communities? Many of the complex interactions observed in macro-ecosystems exist in the microbial world; microbes show a plethora of dispersal strategies[50,51], life-history tradeoffs involving lag times, survival probabilities, growth rates and yields[52–54], as well as social interactions including chemical signaling, quorum sensing, toxin and viral warfare[12,55]. The effects of these factors on the development of spatially structured communities could easily be investigated by varying the microbial species and strains which compete in our experimental setup. Interestingly, we note that

recent high-throughput macroscopic studies of growing colonies of bacteria extracted from soil arrived at a similar conclusion to ours concerning the importance of variation in founder cell lag times for eventual competitive success[40]; although for soil bacteria the situation appears to be more complex, since lag times were dependent on initial cell density[40]. More generally, natural microbial communities often show extremely high levels of species diversity, and as yet, we lack basic fundamental understanding of how this diversity arises and is maintained, and what functional role it may play. Well-controlled laboratory experiments, in conjunction with ecological theory, are essential if we are to change this state of affairs[13].

## Experimental Methods

### *Bacterial strains and growth conditions*

Two strains of *E. coli* MG1655 were used in our experiments, one carrying a cyan fluorescent protein reporter construct and the other a yellow fluorescent protein reporter construct. These strains were made by P1 transduction from strain MRR of Elowitz et al.[56] into an MG1655 background. The reporter constructs are integrated into the *E. coli* genome at positions on either side of the origin of replication (equidistant from the origin) and are under the control of the constitutive $\lambda P_R$ promoter[56]. Separate overnight cultures for each strain were prepared by transfer of a single isogenic plate colony (themselves sourced from from freezer stocks (LB + 30% glycerol)) into 5 ml $M9$ media, supplemented with glucose (0.2%) and casamino acids (0.4%) (all further references to M9 include these supplements) and incubated for $\sim 16$ hours at $37°C$, $200rpm$, where they reached the stationary phase. Growth curves obtained from plate reader data showed no significant difference in growth rates between the two strains.

For experiments using founder cells in the exponential growth phase, a $10^{-3}$ dilution was performed on each strain overnight into fresh $M9$ media, and cells were grown to an optical density $OD_{600nm} \cong 0.3$. Heat-shocked cells were prepared by pipetting 1.5 ml of stationary phase overnight culture into an eppendorf, and placing it in a 50°C heat-block for 15 min. Liquid cultures were mixed at a 1 : 19 (CFP:YFP) ratio, gently vortexed, and diluted to the target optical density (which determined the resulting founder cell density on the surface) using fresh $M9$ media.

In a typical experiment we obtain between 20 and 100 red patches per agarose slab (see "sample preparation" below), depending on the initial cell density. Any cases where patches arising from two separate red founder cells share an interface were disgarded in our analysis.

### *Sample preparation*

A sterile 55 mm x 25 mm x 2.4 mm perspex slide with a 33 mm x 10 mm hole was lightly fixed to a standard glass microscope slide using petroleum jelly, creating a 792 $\mu$l well. Molten 3% M9 agarose was pipetted into the cavity and a microscope coverslip used to flatten the surface. Once the agarose had solidified, the coverslip was carefully removed, revealing an agaroose slab. 1 $\mu$l of diluted mixed culture was pipetted three quarters up the length of the agarose, and the slide held at an angle so liquid culture would run the length of the surface.

After the liquid culture had been fully absorbed, a clean coverslip was carefully placed over the agarose and sealed to the perspex frame using VALAP[57]; the perspex frame was then also sealed to the microscope slide to ensure air tightness.

For cell lag-time experiments, the perspex slide was replaced with a Gene Frame (Thermo Scientific), a disposable, double-sided adhesive plastic frame with volume 125 $\mu$l[58]. The cell mixing ratio was 1 : 1, and cultures were diluted to an appropriate optical density to maximise the number of cells in a single field of view.

### *Microscopy analysis of dual-fluorescence competition experiments*

In our experiments involving mixtures of CFP and YFP-expressing cells, image acquisition was performed using fluorescent microscopy with filters appropriate for detection of either CFP or YFP. An inverted Nikon Ti Eclipse epifluorescent microscope, with 20x objective (NA=0.75 or 0.5) and CoolSNAP $HG^2$ (Photometrics) CCD camera at 2x2 binning were used for all samples. Excitation light was from an *Hg* lamp, passed through Chroma EYFP and ECFP filter sets. Automatic shutters controlled by MetaMorph (Molecular Devices) limited sample exposure to excitation light. A motorised stage (Prior Scientific) facilitated a precise raster scan of the sample, so relative positions of seed cells were accurately known. Following identification of seed cell positions ('day one'), the sample was placed in an airtight container and statically incubated overnight at $30^oC$, before repeating the imaging process ('day two') to record the resulting colonies.

### *Timelapse microscopy*

Timelapse microscopy was used to study the growth of microcolonies prior to collision; here only a single strain was used. All samples were incubated at $32^oC$ during image acquisition. Fluorescence and phase contrast time-lapse microscopy was performed on an upright Nikon E800 epifluorescent microscope with a 100x objective (Nikon, NA=1.3, Ph3), and CCD camera (QImaging Retiga 2000R) at 1x1 binning. Excitation light was

provided by an *Hg* lamp passed through appropriate filter sets. The microscope's XYZ-stage and shutters were controlled via $\mu$Manager[59], and image acquisition automated using the inbuilt 'OughtaFocus' autofocus algorithm. Multiple fields of view were observed in time by saving numerous xy stage coordinates in the software.

### *Image analysis*

Images were thresholded in ImageJ[60] and multiple fields of view were stitched together to form a complete, high resolution montage of the entire surface from both day one and two. The Voronoi map was generated in MATLAB using the built-in 'Voronoi' plugin, before being overlaid with a montage image of CFP cells so Voronoi polygons generated by CFP cells could be identified. The CFP colonies and Voronoi polygons were then paired by identifying overlapping objects in the two images, using routines written in MATLAB ® (2012a,The MathWorks).

For cell lag-times, phase contrast time-lapse movies of dividing cells were manually checked for division times using CellCounter in ImageJ, and corresponding fluorescent images used to determine if the cell expressed CFP or YFP.

### *Computation of Fourier descriptors*

The complex Fourier Descriptor (FD) method provides a convenient way to characterize Voronoi patch shapes. FDs are commonly used in shape recognition analysis[47,61]. A complete description of the boundary of the shape in frequency space is captured by taking the Fourier Transform of the two-dimensional boundary coordinates, expressed as a real-complex number pair. This analysis results in a list of Fourier descriptor magnitudes corresponding to a given shape. Here, higher frequency terms (higher order FDs) describe smaller features of the shape, while lower frequency terms describe larger, more coarse-grained features. The FD spectrum of a shape is translation, rotation and scale invariant.

To compute the Fourier descriptor spectra of our Voronoi patches, patch-boundary pixel coordinates were extracted in MATLAB and ordered so they formed a closed loop of $M$ pixels. Vectors were created to store the coordinates $x_m$ and $y_m$ of each boundary pixel (where $m$ denotes the index in the vector of boundary pixels for a given patch). Since an even number of boundary points is needed in the discrete fast fourier transform algorithm[47], the last boundary coordinate was duplicated if necessary.

The real and imaginary parts of the Fourier descriptors, $a_n$ and $b_n$, were calculated from the boundary coordinates using:

$$a_n + ib_n = \sum_{m=-M/2}^{M/2} (x_m + iy_m)\left(\cos\frac{2\pi nm}{N} - i\sin\frac{2\pi nm}{N}\right) \quad (2)$$

where $n$ is the descriptor number and $N$ the total number of descriptors. We then obtained the Fourier descriptor magnitude $f_n$ for each index $n$, using $f_n = (a_n^2 + b_n^2)^{1/2}$. Descriptors of order $|n| > 25$ were ignored in adherence to the Nyquist frequency to avoid artefacts in the data.[61]. The list of $f_n$ values for each Voronoi patch was used to characterize its shape.

### *Quantifying differences in Voronoi patch shape using Fourier descriptors*

To determine if there was a difference between Fourier signatures for each Voronoi polygon associated with a loser or winner progenitor cell, Multidimensional Scaling Analysis was used. Pairwise Euclidean distances between each Fourier spectra were used to build a dissimilarity matrix, quantifying the difference in shape between pairs of Voronoi polygons associated with a given experiment. Note that in this analysis we only included patches which fell into either the top or bottom 10% of the winner index distribution (i.e. "winners" or "losers"). A 2d projection of the dissimilarity matrix was created in MATLAB, and the points colour-coded by their status as either winners or losers. An MDS plot was then generated from this 2d projection, in which each point represents an individual Voronoi polygon and the distance between any pair of points represents the difference in their shape. To analyse the statistical significance of the apparent clustering visible in these plots (Fig. 6), we used PERMANOVA, implemented in the software Primer[48]. PERMANOVA analysis involves making multiple permutations of the dataset, randomly assigning colour labels. For each permutation, the average distance between points *within* and *between* colour sets is computed, and a distribution is computed for the ratio of these quantities. Comparing the ratio computed for the actual (non-permuted) dataset with this distribution allows one to assign a statistical significance to the apparent clustering seen in the MDS plot.

## Computer simulation methods

Our computer simulations used a 2d grid of 500×500 spatial lattice points, as described in the main text. We assumed that an individual bacterium occupied one lattice site, and bacteria were not allowed to overlap.

First, seed-cell coordinates were generated via a random number generator. From this, a list of cells was created (henceforth referred to as the 'cell list'), each with an index number (which later was used to index the cell lineage). In our simulations with lag times, these were sampled from the experimental lag-time distributions and assigned to seed cells at random; the cell-list was then sorted in ascending order by these lag-times. If no lagtime was used, then division times were assigned instead, picked from a uniform distribution with range

18 min-22 min, and the cell list sorted by the division times. This range was determined from area growth rates derived from time-lapse movies of isolated microcolonies.

Simulation updates were performed at each timestep as described in the main text. Each timestep consisted of WHAT? DID WE SELECT A CELL AT RANDOM? HOW MANY TIMES  WHAT WAS THE TIMESTEP LENGTH?

I THINK WE NEED SOME MORE DETAILS OF THE SIMULATIONS HERE, IF POSSIBLE A COMPLETE DESCRIPTION SO SOMEONE COULD REPEAT THEM

If a mother cell tried to place a daughter cell beyond the boundary edge, it was allowed, but the new cell was not tracked. This way, the edges were treated as open, and did not confine growth. This is similar to the experimental set-up, where a microscope has a finite field of view which colonies at the edges can grow beyond. However, because we did not then know the true area of colonies that touched the edge of our simulation 'field of view', these colonies were not used in analysis.

**Acknowledgements**

We thank P. Cicuta, P. Clegg, D. Dell'Arciprete, A. McVey, G. Melaugh, W. Poon and B. Waclaw for helpful discussions, A. Dawson for assistance in the lab, S. L. Black for making the *E. coli* strains used in these experiments, and the Elowitz lab (CalTech) for supplying strains containing the fluorescent reporter constructs. DPL was funded by an EPSRC DTA studentship and RJA by a Royal Society University Research Fellowship. This work was partially supported by EPSRC under grant EP/J007401/1 and by the Human Frontiers Science Program under grant RGY0081/2012 .

[1] Tilman D. Competition and biodiversity in spatially structured habitats. Ecology. 1994;75:2–16.

[2] Crowley DN P H McLetchie. Trade-offs and spatial life-history strategies in classical metapopulations. Am Nat. 2002;159:190–208.

[3] Ben-Ja cob E, I C, Levine H. Cooperative self-organization of microorganisms. Adv Phys. 2000;49:395–554.

[4] Reichenbach T, Mobilia M, Frey E. Mobility promotes and jeopardises biodiversity in rock-paper-scissors games. Nature. 2007;448:1046–1049.

[5] Malchow H, Petrovskii SV, Venturino E. Spatiotemporal patterns in ecology and epidemiology. Chapman & Hall / CRC, Boca Raton, FL.; 2008.

[6] Court SJ, Blythe RB, Allen RJ. Parasites on parasites: coupled fluctuations in stacked contact processes. Europhys Lett. 2013;101:50001.

[7] Venegas-Ortiz J, Allen RJ, Evans MR. Speed of invasion of an expanding population by a horizontally-transmitted trait. Genetics. 2014;196:497–507.

[8] Turner MG. Landscape ecology in North America: past, present, and future. Ecology. 2005;86:1967–1974.

[9] Stoll P, Bergius E. Pattern and process : competition causes regular spacing of individuals within plant populations. J Ecol. 2005;p. 395–403.

[10] Lawler S, Morin P. Food-web architecture and population-dynamics in laboratory microcosms of protists. Am Nat. 1993;141:675–686.

[11] Holyoak M, Lawler S. The contribution of laboratory experiments on protists to understanding population and metapopulation dynamics. Adv Ecol Res. 2005;37:245–271.

[12] West SA, Diggle SP, Buckling A, Gardner A, Griffin AS. The social lives of microbes. Annu Rev Ecol Evol Syst. 2007;38:53–77.

[13] Prosser J, Bohannan B, Curtis T, Ellis R, Firestone M, Freckleton R, et al. Essay - The role of ecological theory in microbial ecology. Nat Rev Microbiol. 2007;5:384–392.

[14] Kerr B, Neuhauser C, Bohannan BJ, Dean AM. Local migration promotes competitive restraint in a host-pathogen 'tragedy of the commons'. Nature. 2006;442:75–78.

[15] Kerr B, A RM, Feldman MW, Bohannan BJM. Local dispersal promotes biodiversity in a real-life game of rock-paper-scissors. Nature. 2002;418:171–174.

[16] Chao L, Levin BR. Structured habitats and the evolution of anticompetitor toxins in bacteria. P Natl Acad Sci USA. 1981 Oct;78(10):6324–8. Available from: `http://www.pubmedcentral.nih.gov/articlerender.fcgi?artid=349031\&tool=pmcentrez\&rendertype=abstract`.

[17] Zhang Q, Lambert G, Liao D, Kim H, Robin K, Tung C, et al. Acceleration of emergence of bacterial antibiotic resistance in connected micro environments. Science. 2011;333:1764–1767.

[18] Greulich P, Waclaw B, Allen RJ. Mutational Pathway Determines Whether Drug Gradients Accelerate Evolution of Drug-Resistant Cells. Phys Rev Lett. 2012;109:088101.

[19] Hermsen R, Deris JB, Hwa T. On the rapidity of antibiotic resistance evolution facilitated by a concentration gradient. P Natl Acad Sci USA. 2012;109:10775–10780.

[20] Hallatsheck O, Nelson DR. Life at the Front of an Expending Population. Evolution. 2009;64:193–206.

[21] Hallatschek O, Hersen P, Ramanathan S, Nelson DR. Genetic drift at expanding frontiers promotes gene segregation. P Natl Acad Sci USA. 2007 dec;104(50):19926–30. Available from: `http://www.pubmedcentral.nih.gov/articlerender.fcgi?artid=2148399\&tool=pmcentrez\&rendertype=abstract`.

[22] Korolev K, Muller M, Karahan N, Murray A, Hallatschek O, Nelson D. Selective sweeps in growing microbial colonies. Phys Biol. 2012;9:026008.

[23] Brunet E, Derrida B. Shift in the velocity of a front due to a cutoff. Phys Rev E. 1997;56:2597–2604.

[24] Hallatschek O. The noisy edge of traveling waves. P Natl Acad Sci USA. 2011;108:1783–1787.

[25] Shapiro J, Hsu C. *Escherichia coli* K-12 cell-cell interactions seen by time-lapse video. J Bacteriol. 1989;171:5963–5974.

[26] Cho HJ, Jonsson H, Campbell K, Melke P, Williams JW, Jedynak B, et al. Self-organization in high-density bacterial colonies: Efficient crowd control. PLOS Biol.

2007;5(11):2614–2623.

[27] Volfson D, Cookson S, Hasty J, Tsimring LS. Biomechanical ordering of dense cell populations. P Natl Acad Sci USA. 2008;105(40):15346–15351.

[28] Rudge T, Steiner P. Computational modeling of synthetic microbial biofilms. ACS Synth Biol. 2012;Available from: http://pubs.acs.org/doi/abs/10.1021/sb300031n.

[29] Boyer D, Mather W, Mondragón-Palomino O, Orozco-Fuentes S, Danino T, Hasty J, et al. Buckling instability in ordered bacterial colonies. Phys Biol. 2011;8:026008.

[30] Farrell FDC, Hallatschek O, Marenduzzo D, Waclaw B. Mechanically-driven growth of quasi-two dimensional bacterial colonies. Phys Rev Lett. 2013;111.

[31] Grant M, Waclaw B, Allen RJ, Cicuta P. The role of mechanical forces in the planar-to-bulk transition in growing *Escherichia coli* microcolonies. J R Soc Interface. 2014;11.

[32] Rudge TJ, Federici F, Steiner PJ, Kan A, Haseloff J. Cell Polarity-Driven Instability Generates Self-Organized, Fractal Patterning of Cell Layers. ACS Synth Biol. 2013 Jun;Available from: http://www.ncbi.nlm.nih.gov/pubmed/23688051.

[33] Armstrong RA. The effect of rock surface aspect on growth, size structure and competition in the lichen *Rhizocarpon geographicum*, volume = 48, year = 2002,. Environ Exper Bot;p. 187–194.

[34] Steneck RS, Hacker SD, Dethier MN. Mechanisms of competitive dominance between crustose corralling algae: an herbivore-mediated competitive reversal. Ecology. 2002;48:938–950.

[35] McLetchie DN, Garcìa-Ramos G, Crowley PH. Local sex-ratio dynamics: a model for the dioecious liverwort *Marchantia inflexa*. Evol Ecol. 2002;15:231–254.

[36] Sale PF. Maintenance of high diversity in coral reef fish communities. Am Nat. 1977;155:485–496.

[37] Crowley PH, David HM, Ensminger AL, Fuselier LC, Kasi Jackson J, McLetchie DN. A general model of local competition for space. Ecol Lett. 2005;8:176–188.

[38] Aurenhammer F. Voronoi diagrams—a survey of a fundamental geometric data structure. ACM Comput Surv. 1991 sep;23(3):345–405. Available from: http://portal.acm.org/citation.cfm?doid=116873.116880.

[39] Ingraham JL, Maaloe O, Neidhardt FC. Growth of the bacterial cell. Sinauer Associates; 1983.

[40] Ernebjerg M, Kishony R. Distinct growth strategies of soil bacteria as revealed by large-scale colony tracking. Appl Environ Microb. 2012 mar;78(5):1345–52. Available from: http://www.pubmedcentral.nih.gov/articlerender.fcgi?artid=3294487\&tool=pmcentrez\&rendertype=abstract.

[41] I LR, O G, O F, I R, D S, H S, et al. Automated imaging with ScanLag reveals previously undetectable bacterial growth phenotypes. Nat Methods. 2010;7:737–739.

[42] J B, George S, Z K. Parameter estimation for the distribution of single cell lag times. J Theor Biol. 2009;258:24–30.

[43] D'Arrigo M. Indirect measurement of the lag time distribution of single cells of Listeria innocua in food. Appl Environ Microb. 2006;72(4):2533–2538. Available from: http://aem.asm.org/content/72/4/2533.short.

[44] Métris a, George SM, Mackey BM, Baranyi J. Modeling the variability of single-cell lag times for Listeria innocua populations after sublethal and lethal heat treatments. Appl Environ Microb. 2008 nov;74(22):6949–55. Available from: http://www.pubmedcentral.nih.gov/articlerender.fcgi?artid=2583480\&tool=pmcentrez\&rendertype=abstract.

[45] Niven GW, Morton JS, Fuks T, Mackey BM. Influence of environmental stress on distributions of times to first division in Escherichia coli populations, as determined by digital-image analysis of individual cells. Appl Environ Microb. 2008 Jun;74(12):3757–63. Available from: http://www.pubmedcentral.nih.gov/articlerender.fcgi?artid=2446540\&tool=pmcentrez\&rendertype=abstract.

[46] Madigan MT, Martinko JM, Bender KS, Buckley DH, Stahl DA. Brock biology of microorganisms. Thirteenth ed. Pearson Education; 2012.

[47] Gonzalez RC, Woods RE. Digital Image Processing. Addison-Wesley Publishing Company; 1992.

[48] PERMANOVA+ for PRIMER: Guide to Software and Statistical Methods;.

[49] ;. Correlating lag times of individual cells with winner index values is not possible in our experiments, due to insufficient objective resolution.

[50] van Ditmarsch D, Boyle KE, Sakhtah H, Oyler JE, Nadell CD, Déziel E, et al. Convergent Evolution of Hyperswarming Leads to Impaired Biofilm Formation in Pathogenic Bacteria. Cell Reports. 2013 Aug;p. 1–12. Available from: http://linkinghub.elsevier.com/retrieve/pii/S2211124713003884.

[51] Shapiro J. The significances of bacterial colony patterns. Bioessays. 1995;17(i). Available from: http://onlinelibrary.wiley.com/doi/10.1002/bies.950170706/abstract.

[52] Ishikuri S, Hattori T. Analysis of Colony Forming Curves of Soil Bacteria. Soil Sci Plant Nutr. 1987 sep;33(3):355–362. Available from: http://www.tandfonline.com/doi/abs/10.1080/00380768.1987.10557581.

[53] Lewis K. Persister cells, dormancy and infectious disease. Nat Rev Microbiol. 2007;5:48–56.

[54] Kreft JU. Biofilms promote altruism. Microbiol - SGM. 2004;150:2751–2760.

[55] Hibbing M, Fuqua C. Bacterial competition: surviving and thriving in the microbial jungle. Nat Rev Microbiol. 2009;8(1):15–25. Available from: http://www.nature.com/nrmicro/journal/vaop/ncurrent/full/nrmicro2259.html.

[56] Elowitz M, Levine A, Siggia E, Swain P. Stochastic gene expression in a single cell. Science. 2002;297:1183–1186.

[57] Valap. Cold Spring Harbor Protocols. 2007 Feb;2007(2):pdb.rec10885–pdb.rec10885. Available from: \{http://cshprotocols.cshlp.org/content/2007/2/pdb.rec10885.short\}http://www.cshprotocols.org/cgi/doi/10.1101/pdb.rec10885.

[58] de Jong I, Beilharz K, Kuipers O, Veening J. Live Cell Imaging of *Bacillus subtilis* and *Streptococcus pneumoniae* using Automated Time-lapse Microscopy. J Vis Exp. 2005;53:176–188.

[59] Edelstein A, Amodaj N, Hoover K, Vale R, Stuurman N. Computer control of microscopes using Manager. Current protocols in molecular biology / edited by Frederick M Ausubel [et al]. 2010 Oct;Chapter 14(October):Unit14.20. Available from: http://www.pubmedcentral.nih.gov/articlerender.fcgi?artid=3065365\&tool=pmcentrez\&rendertype=abstract.

[60] Schneider Ca, Rasband WS, Eliceiri KW. NIH Image to ImageJ: 25 years of image analysis. Nature Methods. 2012 Jun;9(7):671–675. Available from: http://www.nature.com/doifinder/10.1038/nmeth.2089.

[61] Rice KP, Saunders AE, Stoykovich MP. Classifying the Shape of Colloidal Nanocrystals by Complex Fourier Descriptor Analysis. Cryst Growth Des. 2012 Feb;12(2):825–831. Available from: http://pubs.acs.org/doi/abs/10.1021/cg201156q.